

Applying the Generalized Compass Operator for Image Dominant Orientation Estimation

Tatyana Kislitsyna¹ and Ivan Kholopov¹

¹ Ryazan State Radio Engineering University named after V.F. Utkin (RSREU), Gagarina, 59/1, Ryazan, 390005, Russia

Abstract

Evaluation of the orientation of objects on frames from digital cameras is one of the problems of intelligent image analysis and processing. In this paper, we focus on the two-stage algorithm for image dominant orientation using first rough estimation of orientation angle through principal component analysis of gradient covariance matrix and second more accurate orientation estimation using the generalized compass operator. We compared two types masks of compass operator – Prewitt-like and extended Prewitt-like – for orientation estimation task. We demonstrated that for extended Prewitt-like mask with a size of 5×5 pixels using the generalized compass operator provides an estimation error of the dominant direction no more than 1° compared with methods, based on principal component analysis technique.

Keywords 1

Image dominant orientation, generalized compass operator, Prewitt operator, gradient.

1. Introduction

Image dominant orientation analysis appears in many different contexts in computer vision, image analysis, feature extraction, and pattern recognition, because oriented edges and lines are important image features for both human perception and machine processing. Orientation analysis is widely employed in edge and line detection, which is an important step in object detection and recognition [1], segmentation, texture analysis, and fingerprint classification [2].

For angular orientations that are multiples of $\pi/4$, well-known edge detection operators are Roberts, Prewitt, Sobel, Kirsch, and Schar. The Nevatia-Babu [3] operator is an example of a generalized compass operator, that allows to select edges, for an arbitrary angular orientation of objects on an image. In this case, all the listed edge detection operators are only a tool for the algorithm for selecting edges of a given angular orientation. A powerful and frequently used approach for edge elements that form straight lines in an image is based on the concept of Hough (or Radon) transformation, that maps a points of the straight line in an image into a single point in (R, θ) Hough (or Radon) space, where R is the distance of each straight edge pixel from the origin, and θ is the edge orientation angle. But efficiency of the Hough transform is dependent on the quality of the input data, and its computational complexity is $O(N^4)$, where the size of the image is $O(N^2)$. The variants of the Hough transform for line detection with $O(N^3 \log N)$ are also known, but their computational complexity is high as well. For this reason, methods for estimating the angular orientation of objects that have less computational complexity are needed for practical application.

2. Related work

There are several approaches to extract the orientation feature of images: ideal edge or line profiles detection [4, 5], matched filter approaches, spectral or wavelet estimation methods [6, 7].

GraphiCon 2022: 32nd International Conference on Computer Graphics and Vision, September 19-22, 2022,

Ryazan State Radio Engineering University named after V.F. Utkin, Ryazan, Russia

EMAIL: stroikova.t.s@rsreu.ru (T. Kislitsyna); kholopov.i.s@rsreu.ru (I. Kholopov)

ORCID: 0000-0003-0374-8316 (T. Kislitsyna); 0000-0001-5220-0811 (I. Kholopov)



© 2022 Copyright for this paper by its authors.

Use permitted under Creative Commons License Attribution 4.0 International (CC BY 4.0).

But the accuracy of these methods is limited by using the limited number of fixed possible orientations [1].

For dominant orientation estimation, the approaches based on averaging squared gradients or principal component analysis (PCA) of gradient covariance matrix [8, 9] are often used. Local orientation estimation may be based on a combination of two well-known techniques: PCA, which at its core uses the singular value decomposition (SVD), and the multiscale pyramid decomposition. This orientation estimation method works well in terms of both robustness and accuracy [8].

PCA technique also can be based on the analysis of image gradients field and forming of scattering ellipse [10, 11]. The large axis of the scattering ellipse of the gradients field coincided with the line of orthogonal regression, and the slope angle α is taken as the dominant orientation of the image.

Convolutional neural networks (CNN) are one of the most effective tools in the modern computer vision. They are also used for tasks of detecting the orientation angle of user digital photo images [12-14] automatically. In simpler dataset collections including outdoor scenes, CNN reaches an accuracy higher than 98%, which can be obtained by humans. But one of the main disadvantages of deep neural networks is that the network must be very deep to reach good accuracy [14]. To reduce the complexity of the network the size of the input image and the number of convolution layers should be reduced.

The aim of this work is the development of the two-stage algorithm for image dominant orientation estimation: rough dominant orientation estimation using PCA of gradient covariance matrix at the first stage and its subsequent refinement at the second stage by fixed-step brute-force method using generalized compass operator.

3. Examples of generalized compass operators

3.1. The Prewitt-like generalized compass operator

If the area of the image, on which the gradient operator is calculated, is represented by analogy with [15], then we can take into consideration the Prewitt-like compass operator for required angle α [16]. The matrix \mathbf{M} elements of the operator can be calculated using the following expression:

$$M_{ij} = \begin{cases} s|1 + 2y_0 - (y_1 + y_3)|, & \text{if } b_1 \ \& \ b_3 = 1, \\ s|1 + 2x_0 - (x_2 + x_4)|, & \text{if } b_2 \ \& \ b_4 = 1, \\ s|1 - (y_1 - y_0)(x_4 - x_0)|, & \text{if } b_1 \ \& \ b_4 = 1, \\ s|1 - (y_0 + 1 - y_1)(x_2 - x_0)|, & \text{if } b_1 \ \& \ b_2 = 1, \\ s|1 - (x_0 + 1 - x_2)(y_0 + 1 - y_3)|, & \text{if } b_2 \ \& \ b_3 = 1, \\ s|(y_0 + 1 - x_4)(y_0 + 1 - y_3)|, & \text{if } b_3 \ \& \ b_4 = 1, \\ 0, & \text{if } b_1 \ \& \ b_2 \ \& \ b_3 \ \& \ b_4 = 1, \\ s, & \text{if there are no intersections.} \end{cases} \tag{1}$$

where $s = \text{sign}(kX - Y)$, b_l , b_t , b_r , and b_b are binary features determining the fact of the intersection of the straight line $y = kx$, $k = \text{tg}\alpha$, with the left, top, right, and bottom boundaries sides of the unit pixel square [16]:

$$\begin{aligned} b_l &= \begin{cases} 1, & y_0 \leq y_l \leq y_0 + 1, \text{ where } y_l = kx_0, \\ 0, & \text{otherwise;} \end{cases} \\ b_t &= \begin{cases} 1, & x_0 \leq x_t \leq x_0 + 1, \text{ where } x_t = (y_0 + 1) / k, \\ 0, & \text{otherwise;} \end{cases} \\ b_r &= \begin{cases} 1, & y_0 \leq y_r \leq y_0 + 1, \text{ where } y_r = k(x_0 + 1), \\ 0, & \text{otherwise;} \end{cases} \\ b_b &= \begin{cases} 1, & x_0 \leq x_b \leq x_0 + 1, \text{ where } x_b = y_0 / k, \\ 0, & \text{otherwise.} \end{cases} \end{aligned} \tag{2}$$

The ampersand "&" operator in (1) denotes the logic operator "AND", $x_0 = X - 0.5$ and $y_0 = Y - 0.5$ are the coordinates of the lower left pixel corner with center (X, Y) .

3.2. Extended Prewitt-like generalized compass operator

As follows from (1), weights of \mathbf{M} kernel do not exceed 1 in absolute value. At the same time, it is known [17, 18] that the presence of weight coefficients in the filter mask with an absolute value greater than 1 leads to an additional emphasis on "strong" edges with a high gradient value [19, 20].

For forming a generalized compass operator based on extended [17, 18] Prewitt kernels (5×5 , 7×7 , 9×9), represent the weights of the extended Prewitt operator mask for vertical derivative calculation as the z -coordinates (Figure 1) of the canonical equation of the plane $z = f(x, y)$:

$$n_x x + n_y y + n_z z + C = 0,$$

where $\mathbf{n} = [n_x, n_y, n_z]^T$ is a normal vector to the plane. In this case (see Figure 1), the line l of the intersection of the plane P and the plane Oxy passes through a point with pixel coordinates $(0, 0)$, so constant $C = 0$.

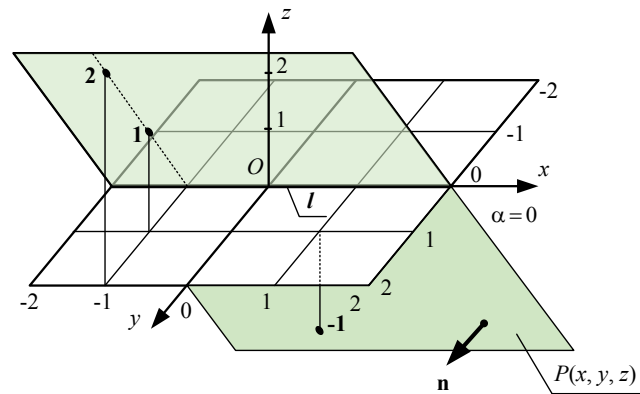


Figure 1: Plane representation of extended Prewitt operator kernel for vertical derivative calculation

Thus, to calculate the elements of the filter mask, the equality

$$\mathbf{M}_{x,y} = z(x, y)$$

is true.

The plane $P(x, y, z)$ from Figure 1 contains a point with coordinates $[x, y, z] = [0, 0, 0]$ and has a normal vector

$$\mathbf{n} = [0, 2^{-0.5}, -2^{-0.5}]^T. \tag{3}$$

In this case, the canonical equation of the plane

$$z = y.$$

To calculate the brightness gradient, the mask of such a filter of size, for example, 5×5 has the form

$$\mathbf{M}_{5 \times 5} = \begin{bmatrix} M_{-2,-2} & M_{-1,-2} & M_{0,-2} & M_{1,-2} & M_{2,-2} \\ M_{-2,-1} & M_{-1,-1} & M_{0,-1} & M_{1,-1} & M_{2,-1} \\ M_{-2,0} & M_{-1,0} & M_{0,0} & M_{1,0} & M_{2,0} \\ M_{-2,1} & M_{-1,1} & M_{0,1} & M_{1,1} & M_{2,1} \\ M_{-2,2} & M_{-1,2} & M_{0,2} & M_{1,2} & M_{2,2} \end{bmatrix} = \begin{bmatrix} -2 & -2 & -2 & -2 & -2 \\ -1 & -1 & -1 & -1 & -1 \\ 0 & 0 & 0 & 0 & 0 \\ 1 & 1 & 1 & 1 & 1 \\ 2 & 2 & 2 & 2 & 2 \end{bmatrix},$$

i.e. it corresponds to the mask of the extended Prewitt operator 5×5 for computing the vertical brightness gradient.

Rotating the plane P around the Oz axis by 90° counterclockwise, i.e. multiplying it by the rotation matrix

$$\mathbf{R}_z(90^\circ) = \begin{bmatrix} \cos(90^\circ) & \sin(90^\circ) & 0 \\ -\sin(90^\circ) & \cos(90^\circ) & 0 \\ 0 & 0 & 1 \end{bmatrix} = \begin{bmatrix} 0 & 1 & 0 \\ -1 & 0 & 0 \\ 0 & 0 & 1 \end{bmatrix},$$

we get the new normal vector

$$\mathbf{n}^* = \mathbf{R}_z(90^\circ) \mathbf{n} = [2^{-0.5}, 0, -2^{-0.5}]^T,$$

new plane equation for angle $\alpha = -90^\circ$

$$z = x,$$

and the mask of the extended Prewitt operator 5×5 for computing the horizontal brightness gradient:

$$\mathbf{M}_{5 \times 5} = \begin{bmatrix} M_{-2,-2} & M_{-1,-2} & M_{0,-2} & M_{1,-2} & M_{2,-2} \\ M_{-2,-1} & M_{-1,-1} & M_{0,-1} & M_{1,-1} & M_{2,-1} \\ M_{-2,0} & M_{-1,0} & M_{0,0} & M_{1,0} & M_{2,0} \\ M_{-2,1} & M_{-1,1} & M_{0,1} & M_{1,1} & M_{2,1} \\ M_{-2,2} & M_{-1,2} & M_{0,2} & M_{1,2} & M_{2,2} \end{bmatrix} = \begin{bmatrix} -2 & -1 & 0 & 1 & 2 \\ -2 & -1 & 0 & 1 & 2 \\ -2 & -1 & 0 & 1 & 2 \\ -2 & -1 & 0 & 1 & 2 \\ -2 & -1 & 0 & 1 & 2 \end{bmatrix}.$$

Thus, to select the image brightness gradient along an arbitrary angular direction α , $-180^\circ \leq \alpha \leq 180^\circ$, it is required (see Figure 2) to form a filter mask, the weight coefficients of which are obtained from the plane equation with the normal vector (3), rotating around the Oz axis by an angle α , while the positive value of this angle is measured in a counterclockwise direction:

$$\begin{aligned} P_\alpha(x, y, z) &= [\mathbf{R}_z(\alpha)\mathbf{n}] \cdot [x, y, z]^T = \\ &= 2^{-0.5}x \sin\alpha + 2^{-0.5}y \cos\alpha - 2^{-0.5}z = 0, \end{aligned}$$

where "." is the dot product designation. In this case, the elements of the filter mask are calculated by the formula

$$M_{x,y}(\alpha) = P_\alpha(x, y, z) = z_\alpha(x, y) = x \sin\alpha + y \cos\alpha. \quad (4)$$

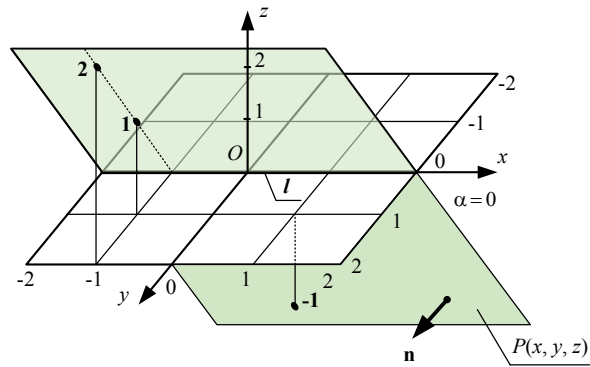


Figure 2: Plane representation of extended Prewitt operator kernel for an arbitrary angular direction α

4. Description of two-stage algorithm for image dominant orientation estimation

We use a generalized compass operator for refinement of the results of PCA [21] according to the following two-stage algorithm (TSA).

1. Pre-filtration: convolution of the initial analyzed image I with Gaussian 2D kernel (we used kernel with $\sigma_g = 5$ pixels) and get I_g image.
2. Calculation of the covariance matrix

$$\mathbf{C} = \begin{bmatrix} \sum g_x^2 & \sum g_x g_y \\ \sum g_x g_y & \sum g_y^2 \end{bmatrix},$$

where g_x and g_y are derivatives of image I_g in x and y direction, respectively.

3. Stage 1: estimation of the dominant direction α_1 as the direction of the first singular vector of \mathbf{C} [8] after its singular value decomposition.
4. Stage 2: refinement of the α_1 value by fixed step $\delta\alpha$ brute-force method from $\alpha_1 - 0.5\Delta\alpha$ to $\alpha_1 + 0.5\Delta\alpha$ using generalized compass operator, where $\Delta\alpha$ is the search range, and do following:
 - for angle $\alpha_i = \alpha_1 - 0.5\Delta\alpha + i\delta\alpha$ calculate generalized compass operator mask $\mathbf{M}(\alpha_i)$ using formula (1) or (4);
 - calculate convolution $\mathbf{I}_{conv_i} = \mathbf{I}_g \otimes \mathbf{M}(\alpha_i)$;
 - calculate the variance var_i of \mathbf{I}_{conv_i} ;
 - if current variance var_i is greater than all previous, then new refinement value $\alpha_2 = \alpha_i$.

5. Results and discussion

5.1. Estimation of the tilt of the Learning Tower of Pisa

For the Learning Tower of Pisa image (Figure 3) we compared our approach with the PCA method for the dominant orientation estimation for different standard deviations σ_n of additive white noise. We used $\Delta\alpha = 10^\circ$ interval and $\delta\alpha = 0.05^\circ$ step. The results of the experiment are summarized in Table 1.

As known, the tilt of the tower is currently approximately $\theta = 3.97^\circ$, so the true dominant orientation of the image in Figure 3 we assumed is equal to $\alpha_{\text{true}} = 90 - \theta = 86.03^\circ$.

From Table 1 we see that although TSA is less robust to additive noise compared to PCA, it provides an error in estimating the slope angle of no more than 0.4° for extended Prewitt-like 5×5 pixels compass operator mask (4) and no more than 0.55° – for 3×3 pixels mask. The bold font in the Table 1 indicates the cells, where the absolute error in estimating the angle of inclination does not exceed 1° .

5.2. Examples of applying the two-stage algorithm to images with directional textures

We also applied our algorithm to three images with predominant orientations from [10] (see Figure 4 and Table 2). For example, for image Figure 4, *a*, you can use a naive approach to determine the dominant angular orientation – by manually drawing several straight lines that are parallel to texture lines and estimating their average slope ($\alpha_{\text{naive}} = 60.63^\circ$). For the other two images (Figure 4, *b*, *c*) a similar naive analysis is difficult and we can only state, like the authors [10], that these values quite correspond to the visual estimation results.



Figure 3: Image of the Learning Tower of Pisa

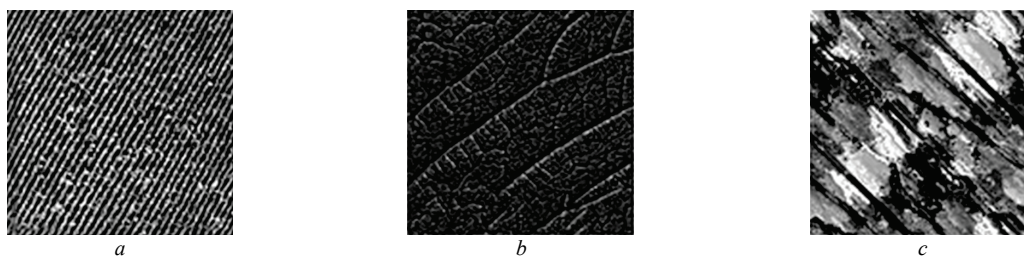


Figure 4: Examples of images with directional textures

From Table 2 we see that for image Figure 4, *a*, TSA approach provides closer to the naive approach estimation of the dominant orientation angle of texture.

Table 1 – The Results of the Tilt Estimation at Different Noise Standard Deviation σ

σ	Asatryan at al. [10], PCA [21]	TSA with mask (1)		TSA with mask (4)	
		3×3 mask	5×5 mask	3×3 mask	5×5 mask
0	85.58°	80.60°	80.60°	86.05°	86.05°
5	85.58°	79.40°	80.60°	85.40°	86.10°
10	85.62°	79.40°	80.70°	85.40°	86.10°
15	85.72°	79.40°	80.70°	85.40°	86.20°
20	85.66°	79.40°	80.80°	85.30°	86.30°
25	85.47°	79.55°	80.95°	85.50°	86.40°

Table 2 – The Results of the Dominant Angular Orientation Estimation for Various Algorithms

Figure 4 image	Asatryan et al. [10]	TSA with 3×3 mask (4)
a	65°	61.55°
b	18°	26.45°
c	136° (-44°)	-43.40°

6. Conclusion

The proposed extended Prewitt-like compass operator makes it possible to select in images contours with a given angular orientation. For a mask with a size of 5×5 pixels, this operator provides to determine the dominant image direction with an absolute error, not exceeding 1°.

7. Acknowledgements

The work was performed as part of the state assignment of the Ministry of Science and Higher Education of the Russian Federation (FSSN-2020-0003).

8. References

- [1] X. Jiang, Extracting image orientation feature by using integration operator, in: Pattern Recognition, volume 40(2), 2007, pp. 705–717.
- [2] C. H. Park, H. Park, Fingerprint classification using fast Fourier transform and nonlinear discriminant analysis, in: Pattern Recognition, volume 38(4), 2005, pp 495–503.
- [3] R. Nevatia, K. R. Babu, Linear feature extraction and description, in: Computer Graphics and image Proc., volume 13, 1980, pp. 257–269.
- [4] D. Ziou, S. A. Tabbone, Edge detection techniques - an overview, in: Pattern Recognition and Image Analysis, volume 8, no. 4, 1998, pp. 537–559.
- [5] R. Kirsch, Computer determination of the constituent structure of biological images, in: Computers and Biomedical Research, volume 4, no. 3, 1971, pp. 315–328.
- [6] T. Yang, J. Ma, S. Huang, Q. Zhao, A new edge detection algorithm using FFT procedure, in: Lecture Notes in Electrical Engineering, volume 278, 2014, pp. 297–304.
- [7] L. Zhang, P. Bao, Edge detection by scale multiplication in wavelet domain, in: Pattern Recognition Letters, volume 23(4), 2002, pp. 1771–1784.
- [8] X. Feng and P. Milanfar, Multiscale principal components analysis for image local orientation estimation, in: Conf. Record of the 36th Asilomar Conf. on Signals, Systems and Computers, volume 1, Pacific Grove, USA, 2002, pp. 478–482.
- [9] X. Zhu, P. Milanfar, Automatic parameter selection for denoising algorithms using a no-reference measure of image content, in: IEEE Trans. on Image Processing, volume 19(12), 2010, pp. 3116–3132.

- [10] D. Asatryan, K. Egiazarian, and V. Kurkchian, Orientation estimation with applications to image analysis and registration, in: *Int. J. "Information Theories and Applications"*, volume 17, no. 4, 2010, pp. 303-311.
- [11] D. G. Asatryan, Gradient-based technique for image structural analysis and applications, in: *Computer Optics*, volume 43, no. 2, 2019, pp. 245–250.
- [12] P. Fischer, A. Dosovitskiy, T. Brox, Image orientation estimation with convolutional networks, in: *Lecture Notes in Computer Science*, 2015, pp. 1–11.
- [13] J. Lee, Y. Jeong, M. Cho, Self-supervised learning of image scale and orientation, in: *Proc. British Machine Vision Virtual Conference*, 2021, pp. 1-14.
- [14] A. Lumini, L. Nanni, L. Scattolaro, G. Maguolo, Image orientation detection by ensembles of Stochastic CNNs, in: *Machine Learning with Applications*, volume 6, 2021, pp. 1–9.
- [15] C. W. Wang, Real time Sobel square edge detector for night vision analysis, in: *Lecture Notes in Computer Science*, no. 4141, 2006, pp. 403–414.
- [16] T. S. Kislitsyna, I. S. Kholopov, Generalized compass operator for edge detection with the required angular orientation, in: *Proceedings 10th Mediterranean Conf. on Embedded Computing*, Budva, Montenegro, 2021, pp. 302-305.
- [17] R. A. R. Lateef, Expansion and implementation of a 3x3 Sobel and Prewitt edge detection filter to a 5x5 dimension filter, in: *J. Baghdad College of Economic sciences University*, volume 18, 2008, pp. 336–348.
- [18] G. Levkine, Prewitt, Sobel and Scharr gradient 5x5 convolution matrices, in: *Image Process. Articles*, Second Draft, 2012.
- [19] J. Canny, A computational approach to edge detection, in: *IEEE Trans. on Pattern Analysis and Machine Intelligence*, volume 8, no. 6, 1986, pp. 679–698.
- [20] R. Deriche, Using Canny's criteria to derive a recursively implemented optimal edge detector, in: *Int. J. Comp. Vision*, volume 1, 1987, pp. 167–187.
- [21] K. V. Mardia, P. E. Jupp, *Directional Statistics*, J. Wiley Sons Ltd, 2000.